of the level employed (MP2, MP3, or MP4), this value—which agrees with McKee's results[4]—should be reliable. Since this barrier is very low, the C_1 forms interconvert rapidly and the NMR spectra reveal only C_s symmetry.[6] Despite the minor energetic changes during this interconversion, a substantial internal reorganization is involved. Not only the H_b distances but also those involving B_2 and B_5 differ appreciably in the transition state (**1a**) C_s from those in C_1 energy minimum (**1b**) (cf. Figure 2).

It seems conclusive: B_5H_{11} prefers an unsymmetrical structure of C_1 symmetry. The apical hydrogen H_b is involved in a "normal" three-center B-H-B bond (see Figure 2) rather than bridging three borons. A factor contributing to this structural preference is indicated by natural population analysis[11] (see Figure 1): In **1a**, the bond order between H_b and the basal borons B_2 and B_5 is significant but rather small (0.14). The stronger interaction of H_b with B_2 in **1b** (bond order 0.34) more than compensates for the reduced overlap to B_5.

IGLO calculations have been applied with great success to help solve carbocation structural problems.[8] This first application to boron compounds underscores the promise of this new approach for similar purposes.

Acknowledgment. We thank the Fonds der Chemischen Industrie, the Deutsche Forschungsgemeinschaft, the Convex Computer Corp., and the Stiftung Volkswagenwerk for support of this work at Erlangen. We thank Prof. W. Kutzelnigg and Dr. M. Schindler for the development of the IGLO program and Dr. Schindler for supplying the Convex version, which was employed at Erlangen and is available for distribution. The IGLO calculations in Bochum were carried out on a Cyber 205 computer, and the MP2 optimization was carried out on an IBM 3090 computer using a vectorized version of the GAUSSIAN 86 program. We also thank D. W. Rankin, N. N. Greenwood, R. A. Beaudet, and a reviewer for helpful comments and the KFA, Jülich, FRG, for computer time.

Registry No. B_5H_{11}, 18433-84-6.

(11) Reed, A. E.; Weinstock, R. B.; Weinhold, F. *J. Chem. Phys.* **1985**, *83*, 735.

Institut für Organische Chemie — **Paul von Ragué Schleyer***
Friedrich-Alexander Universität — **Michael Bühl**
Erlangen-Nürnberg
Henkestrasse 42
D-8520 Erlangen, West Germany

Lehrstuhl für Theoretische Chemie — **Ulrich Fleischer**
Ruhr-Universität Bochum
Universitätsstrasse 150
D-4630 Bochum, West Germany

IBM Wissenschaftliches Zentrum — **Wolfram Koch**
Tiergartenstrasse 15
D-6900 Heidelberg, West Germany

Received August 29, 1989

Thermal Control of Photoreactivity: Room-Temperature Photosubstitution vs 150 K Electron Transfer in $[(dmb)_2Ru(3\text{-}Br\text{-}py)_2](PF_6)_2$

An interesting feature of the photochemistry of ruthenium(II) diimine complexes is the observation of photosubstitution from ^{3}LF states[1-5] and photoredox reactivity from ^{3}MLCT states.[1,6-10]

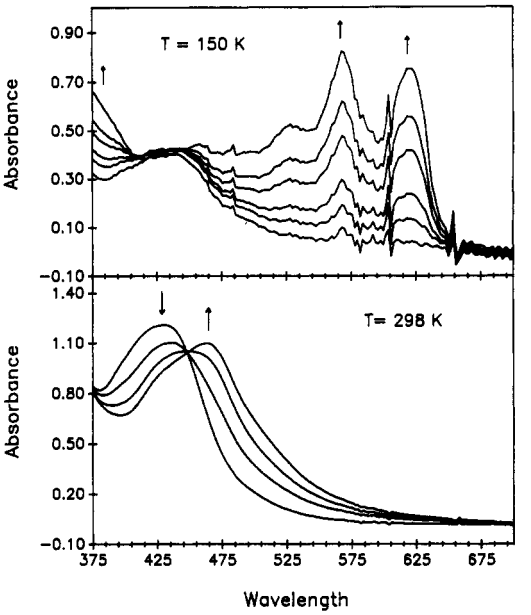

Figure 1. Photolysis of mixtures of $[(dmb)_2Ru(3\text{-}Br\text{-}py)_2](PF_6)_2$ and TMPD (0.05 M) in 4:1 ethanol-methanol at 150 K and 298 K using $\lambda > 450$ nm light from a Xe 150-W arc lamp (PTI). Spectra were taken at 30-s intervals.

Scheme I

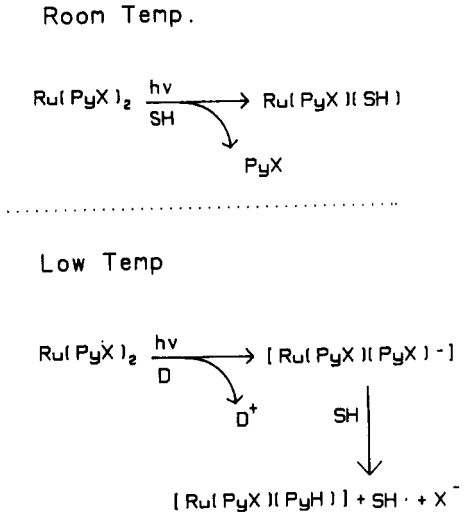

For $[Ru(bpy)_3](PF_6)_2$ in room-temperature acetonitrile solutions, both photoredox reactions and, to a much smaller degree, pho-

(1) For recent reviews see: (a) Kalyanasundaram, K. *Coord. Chem. Rev.* **1982**, *48*, 159. (b) Juris, A.; Balzani, V.; Barigelletti, F.; Campagna, S.; Belser, P.; von Zelewsky, A. *Coord. Chem. Rev.* **1988**, *82*, 85. (c) Meyer, T. J. *Pure Appl. Chem.* **1986**, *58*, 1193. (d) Sutin, N.; Creutz, C. *J. Chem. Educ.* **1983**, *60*, 809-14.

(2) (a) Durham, B.; Caspar, J. V.; Nagle, J. K.; Meyer, T. J. *J. Am. Chem. Soc.* **1982**, *104*, 4803. (b) Durham, B.; Walsh, J. L.; Carter, C. L.; Meyer, T. J. *Inorg. Chem.* **1980**, *19*, 860. (c) Caspar, J. V.; Meyer, T. J. *J. Am. Chem. Soc.* **1983**, *105*, 5583. (d) Caspar, J. V.; Meyer, T. J. *Inorg. Chem.* **1983**, *22*, 2444.

(3) (a) Van Houten, J.; Watts, R. J. *J. Am. Chem. Soc.* **1976**, *98*, 4853. (b) Van Houten, J.; Watts, R. J. *Inorg. Chem.* **1978**, *17*, 3381.

(4) Hoggard, P. E.; Porter, G. B. *J. Am. Chem. Soc.* **1978**, *100*, 1457.

(5) (a) Wacholtz, W. F.; Auerbach, R. A.; Schmehl, R. H.; Ollino, M. A.; Cherry, W. R. *Inorg. Chem.* **1985**, *24*, 1758. (b) Wacholtz, W. F.; Auerbach, R. A.; Schmehl, R. H. *Inorg. Chem.* **1986**, *25*, 227. (c) Wright, D. W.; Corona, B.; Schmehl, R. H. Manuscript in preparation.

(6) Whitten, D. G. *Acc. Chem. Res.* **1980**, *13*, 83.

(7) (a) Meyer, T. J. *Acc. Chem. Res.* **1978**, *11*, 94. (b) Meyer, T. J. *Acc. Chem. Res.* **1989**, *22*, 163.

(8) Prasad, D. R.; Mandal, K.; Hoffman, M. Z. *Coord. Chem. Rev.* **1985**, *64*, 175.

(9) Lee, L. Y. C.; Schanze, K. S.; Giannotti, C.; Whitten, D. G. In *Homogeneous and Heterogeneous Photocatalysis*; NATO ASI Series, Series C; D. Reidel Publ.: Boston, MA, 1986.

(10) Gratzel, M. *Acc. Chem. Res.* **1981**, *14*, 376.

(11) (a) Maidan, R.; Willner, I. *J. Am. Chem. Soc.* **1986**, *108*, 8100. (b) Maidan, R.; Willner, I. *J. Am. Chem. Soc.* **1986**, *108*, 1080. (c) Maidan, R.; Goren, Z.; Becker, J. Y.; Willner, I. *J. Am. Chem. Soc.* **1984**, *106*, 6271.

0020-1669/90/1329-0155$02.50/0

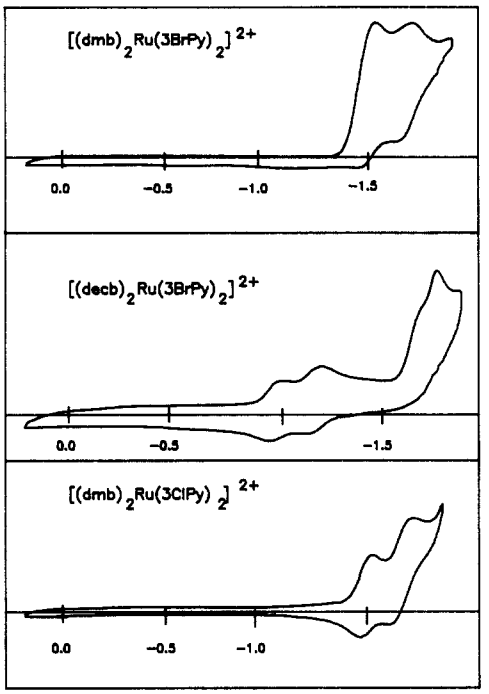

Figure 2. Reductive cyclic voltammograms of $[(dmb)_2Ru(3\text{-}Br\text{-}py)_2](PF_6)_2$, $[(decb)_2Ru(3\text{-}Br\text{-}py)_2](PF_6)_2$ and $[(dmb)_2Ru(3\text{-}Cl\text{-}py)_2](PF_6)_2$ in CH_3CN with tetrabutylammonium hexafluorophosphate as supporting electrolyte at 298 K. Sweep rate = 200 mV/s. Reference = SSCE.

tosubstitution are observed.[1,2] There are, however, numerous ruthenium(II) diimine complexes such as $[(bpy)_2Ru(py)_2](PF_6)_2$ that exhibit efficient photosubstitution at room temperature.[2b,5a,c] At temperatures below 200 K, these complexes exhibit luminescence. The decrease in emission intensity with increasing temperature has been rationalized as resulting from thermally activated internal conversion from the emissive ^{3}MLCT state to a labile ^{3}LF state.[1b,c,3] Thus it should be possible to use temperature cycling to combine low-temperature photoredox chemistry, which acts on a coordinated ligand, with photosubstitution of the ligand at room temperature in a catalytic cycle. Application of this concept to the reductive dehalogenation of 3-bromopyridine (3-Br-py) is presented here. It is shown that $[(dmb)_2Ru(3\text{-}Br\text{-}py)_2](PF_6)_2$ (dmb = 4,4′-dimethyl-2,2′-bipyridine) loses Br^- upon reductive quenching by *N,N,N′,N′*-tetramethylphenylenediamine, TMPD, at 150 K while photosolvation is dominant at room temperature.

Irradiation into the MLCT absorption of $[(dmb)_2Ru(3\text{-}Br\text{-}py)_2](PF_6)_2$ in 4:1 EtOH–MeOH at 150 K results in no net change. Photolysis of deaerated solutions containing the reductive quencher TMPD (0.05 M) results in absorption spectral changes indicating formation of $TMPD^+$ (Figure 1). $TMPD^+$ is not observed when solutions of TMPD alone or mixtures of $[(dmb)_2Ru(py)_2](PF_6)_2$ and TMPD are irradiated at 150 K. The observations are consistent with the low-temperature reactions of Scheme I. The TMPD reduces the excited Ru(II) complex; this is followed by loss of bromide from the reduced complex at a rate that competes with back electron transfer of the Ru(I) complex with $TMPD^+$, resulting in accumulation of $TMPD^+$ in solution. Further evidence supporting the low-temperature mechanism of Scheme I is based on electrochemical results presented below.

Room-temperature photolysis of deaerated ethanol solutions of $[(dmb)_2Ru(3\text{-}Br\text{-}py)_2](PF_6)_2$, either in the presence or in the absence of TMPD, results in the formation of $[(dmb)_2Ru(3\text{-}Br\text{-}py)(EtOH)]^{2+}$. Spectral changes observed are shown in Figure 1; a spectrum identical with the limiting spectrum is observed when the complex $[(dmb)_2Ru(3\text{-}Br\text{-}py)Cl](PF_6)$ is treated with $Ag(BF_4)$ in ethanol. If 3-Br-py (>1 M) is present, the $(3\text{-}Br\text{-}py)_2$ complex is slowly formed at room temperature. The photosubstitution, in combination with the low-temperature photoredox reactivity, completes the cycle for catalytic 3-Br-py dehalogenation.

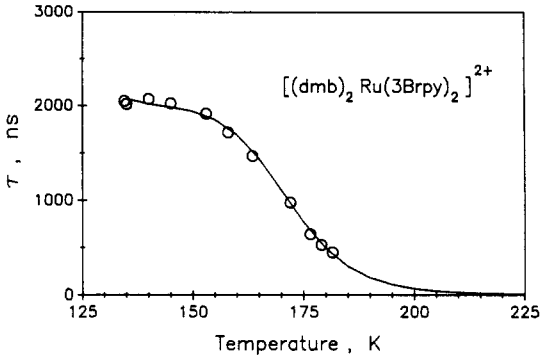

Figure 3. Temperature dependence of luminescence lifetime, τ, of $[(dmb)_2Ru(3\text{-}Br\text{-}py)_2](PF_6)_2$ in 4:1 ethanol–methanol. Solid line represents the best fit for a single activated nonradiative decay path (see text).

To establish the reactivity observed upon low-temperature photoreduction, the room-temperature redox behavior of $[(dmb)_2Ru(3\text{-}Br\text{-}py)_2](PF_6)_2$ was examined. Reduction of halopyridines typically does not occur at potentials positive of −2.0 V vs SCE, but halide loss occurs rapidly following reduction.[12,13] Coordinated bromopyridine in $[(dmb)_2Ru(3\text{-}Br\text{-}py)_2](PF_6)_2$ readily loses Br^- upon reduction in CH_3CN at potentials negative of −1.4 V. Figure 2 shows reductive cyclic voltammograms for three complexes: $[(dmb)_2Ru(3\text{-}Br\text{-}py)_2](PF_6)_2$, $[(decb)_2Ru(3\text{-}Br\text{-}py)_2](PF_6)_2$ and $[(dmb)_2Ru(3\text{-}Cl\text{-}py)_2](PF_6)_2$ (decb = 4,4′-bis(2-carboxyethyl)-2,2′-bipyridine). The first reductive wave of $[(dmb)_2Ru(3\text{-}Br\text{-}py)_2](PF_6)_2$ is irreversible. Bulk electrolysis of the complex in CH_3CN at −1.5 V vs SCE results in $[(dmb)_2Ru(py)_2]^{2+}$ [17] following addition of 2 equiv of electrons. A likely path for this process given the results and literature precedent[12-16] involves halide loss following reduction, yielding an aryl radical that abstracts a hydrogen atom from the solvent. If the spectator ligands are much more easily reduced than the 3-Br-py or if chloropyridine is the target ligand, reduction does not result in facile halide loss. For instance, the first two reductive waves of $[(decb)_2Ru(3\text{-}Br\text{-}py)_2](PF_6)_2$ are reversible, being localized on the decb ligands (Figure 2). The third reductive wave at −1.70 V, clearly irreversible, corresponds to reduction of the coordinated 3-Br-py. Figure 2 also shows that one-electron reduction of $[(dmb)_2Ru(3\text{-}Cl\text{-}py)_2](PF_6)_2$ in CH_3CN is reversible. This may be the result of either slow reaction of the C–Cl bond or the more negative reduction potential of chloropyridine.[12,14] Cyclic voltammograms at slow scan rates (1 mV/s) show that the first complex reduction is still reversible ($i_{p,a}/i_{p,c} \approx 1$), suggesting that thermodynamic effects account for the lack of reactivity.

The efficiency of populating the ^{3}LF state can be determined from the temperature dependence of the luminescence from solutions of $[(dmb)_2Ru(3\text{-}Br\text{-}py)_2](PF_6)_2$. Cooling of 4:1 ethanol:methanol solutions to 180 K results in the appearance of an intense, long-lived emission from the ^{3}MLCT state (λ_{em} = 576 nm at 77 K). Figure 3 shows the temperature dependence of the luminescence lifetime, τ, between 125 and 225 K. The data are fit by assuming the temperature dependence in this region arises from a single thermally activated internal conversion process from the ^{3}MLCT state to a ^{3}LF state.[1,3,5a] The activation barrier from the fit is 2800 cm^{-1}.[18] The efficiency of the internal conversion

(12) Andrieux, C. P.; Blooman, C.; Dumas-Bouchiat, J.-M.; Saveant, J.-M. *J. Am. Chem. Soc.* **1979**, *101*, 3431.
(13) Saveant, J. M. *Acc. Chem. Res.* **1980**, *13*, 323.
(14) Bunnett, J. F. *Acc. Chem. Res.* **1978**, *11*, 413.
(15) Holy, N. L. *Chem. Rev.* **1974**, *74*, 243.
(16) Hawley, M. D. In *Encyclopedia of Electrochemistry of the Elements*; Bard, A. J., Lund, H., Eds.; Dekker: New York, 1980; Vol. XIV, Chapter 3.
(17) The product $[(dmb)_2Ru(py)_2](PF_6)_2$ was identified by cyclic voltammetry, spectrophotometry, and elemental analysis following chromatography on acidic alumina with CH_3CN. The yield of the bis(pyridine) complex recovered ranged from 50% to 70%.

process at these temperatures is given by eq 1, where τ is the

$$\eta_{ic} = 1 - (\tau_T/\tau_{77}) \quad (1)$$

luminescence lifetime at temperature T and τ_{77} is the lifetime at 77 K ($\tau_{77} = (k_r + k_{nr})^{-1}$). At 77 K, the thermally activated population of the ^{3}LF state does not contribute to the relaxation of the ^{3}MLCT state. At 150 K the efficiency for populating the ^{3}LF state is 0.09, while at room temperature (298 K) the efficiency is essentially 1.0 (there is no luminescence). This explanation of nonradiative relaxation is consistent with the observed photochemistry. At low temperatures, photoreactivity is dominated by redox reactions of the ^{3}MLCT state while room-temperature photochemistry results in photosubstitution via the ^{3}LF state.

We are currently examining other complexes that exhibit the crossover between photoredox reactivity and photosubstitution at temperatures closer to room temperature.

Acknowledgment is made to the Louisiana Educational Quality Support Fund, administered by the Louisiana State Board of Regents, for support of this work.

(18) The prefactor of the fit, 1×10^{16} s^{-1} is larger than any reasonable value (upper limit 10^{11}–10^{13}s^{-1}). The simple fitting algorithm used does not include effects on the luminescence lifetime due to changes in the solvent in the 100–125 K region (glass to fluid transition region).[19] The parameters obtained may still be used to determine the magnitude of the thermally activated decay relative to the radiative and nonradiative decay paths of the ^{3}MLCT state.

(19) (a) Juris, A.; Barigelletti, V.; Balzani, V.; Belser, P.; von Zelewsky, A. *Inorg. Chem.* **1985**, 202. (b) Barigelletti, F.; Juris, A.; Balzani, V.; Belser, P.; von Zelewsky, A. *J. Phys. Chem.* **1987**, *21*, 1095.

Department of Chemistry
Tulane University
New Orleans, Louisiana 70118

David W. Wright
Russell H. Schmehl*

Received August 7, 1989

Synthesis and Structural Characterization of $[(MoO)_4O_4(PO_4)_2]^{2-}$: A New Layered Oxide Produced by Hydrothermal Synthesis

In an effort to identify new materials with interesting properties, we have recently employed hydrothermal synthesis techniques to produce oxide lattices containing both octahedral and tetrahedral sites. This has resulted[1,2] in a new group of microporous materials, the stannosilicates, containing octahedral tin(IV) in an oxide lattice with tetrahedrally coordinated silicon. We have now extended this work to include another class of mixed framework oxides consisting of octahedral molybdenum(V) with phosphate tetrahedra. We report herein the first example of a hydrothermal synthesis product from this ternary group, a new layered compound, $[N(C_3H_7)_4(NH_4)][(MoO)_4O_4(PO_4)_2]$, which is made up of extended sheets of Mo_4O_8 cubes linked through corner-sharing phosphate tetrahedra.

When 12.70 g of commercial "molybdic acid" (ammonium dimolybdate, Aldrich, 85% MoO_3 by weight) was dissolved in a phosphoric acid solution (8.14 g of 85% phosphoric acid diluted with 19.76 g of distilled water), a yellowish solution resulted. Addition of tetrapropylammonium bromide (9.40 g, Alfa) produced a smooth gel that was sealed in a 23-mL Teflon-lined autoclave (Parr) and reacted hydrothermally for 2 weeks at 200 °C and autogenous pressure. The resulting red/brown solid (16.25 g, 96% yield based on Mo) was removed and washed repeatedly with water.

(1) Corcoran, Jr., E. W.; Vaughan, D. E. W. *Solid State Ionics* **1989**, *32/33*, 423.

(2) Corcoran, Jr., E. W.; Newsam, J. M.; King, Jr., H. E.; Vaughan, D. E. W. *ACS Symposium Series 398*; American Chemical Society: Washington, DC, 1989; Chapter 41.

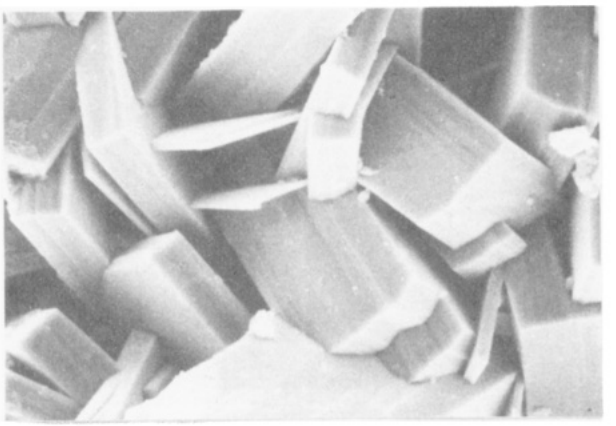

Figure 1. Scanning electron micrograph of the layered compound $[N(C_3H_7)_4(NH_4)][(MoO)_4O_4(PO_4)_2]$, 1575×, showing single crystals of stacked sheets.

Powder X-ray diffraction analysis of the material indicated a single-phase sample had been produced that was indexed by using a tegragonal unit cell having lattice constants of $a = 7.5$ Å and $c = 11.5$ Å. Multiple orders of $00l$ were apparent in the pattern, suggesting a layered topology for the compound. Scanning electron micrographs (Figure 1) supported this argument, showing single crystals approximately 0.2 mm on each edge comprised of stacked rectangular sheets. A suitable crystal was selected for structural characterization[3] by X-ray crystallography, which provided a structural solution (shown in Figure 2) consistent with thermogravimetric and chemical analysis.[4]

The structure of $[(MoO)_4O_4(PO_4)_2]^{2-}$ consists of infinite two-dimensional sheets of Mo_4O_8 cubes, with each cube separated from the next by a corner-sharing phosphate tetrahedron. This results in a regular arrangement of alternating cubes and tetrahedra, in each direction within the $(00l)$ plane, with every cube connected to four others by four phosphate tetrahedra and with each phosphate group linking two cubes. Tetrapropylammonium cations are located within the interlayer space (beneath phosphate tetrahedra) with the nitrogen atoms distributed over two equivalent Wyckoff f sites at 50% occupancy. The ammonium groups, which sit in d positions, are within the layer plane centered in cavities created by four adjacent cubes. The overall lattice structure resembles that of $Cs_3Mo_4P_3O_{16}$,[5] which exhibits the same arrangement of molybdenum cubes as $[(MoO)_4O_4(PO_4)_2]^{2-}$, but, in addition, has two corner-sharing phosphate tetrahedra per cube that join adjacent layers to generate a three-dimensional framework.

The Mo_4O_8 cubes in $[(MoO)_4O_4(PO_4)_2]^{2-}$ (Figure 3) are comprised of four, triply edge-sharing Mo^VO_6 octahedra each having a molybdenyl group (Mo═O, 1.669 (7) Å) in a position

(3) The structure of $[N(C_3H_7)_4(NH_4)][(MoO)_4O_4(PO_4)_2]$ was initially solved and refined in three different space groups ($P2$, $P222$, and $P\bar{4}2m$) with little effect on the molybdenum phosphate network; the cation was disordered in all three space groups. Refinement in $P\bar{4}2m$ resulted in the lowest residuals. Crystal data: tetragonal, $P\bar{4}2m$ (No. 111), $a = 7.512$ (3) Å, $c = 11.384$ (3) Å, $V = 642.4$ (6) Å^3, $Z = 1$, D(calcd) = 2.342 g/cm^3, λ(Mo Kα) = 0.71069 Å, $T = -115$ °C. A Rigaku AFC6R diffractometer, with a graphite monochrometer and a 12-kW rotating anode generator, was used to collect 1316 reflections ($2\theta < 50°$) on a red pyramidal crystal $0.2 \times 0.1 \times 0.1$ mm. Of these, 385 were unique, $R_{int} = 0.021$, and 311 were observed ($I > 3\sigma(I)$). An empirical absorption coefficient, using the program DIFABS (Walker, Stuart, *Acta Crystallogr.* **1983**, *A39*, 158), was applied to the data, which resulted in transmission factors between 0.87 and 1.18. The structure was solved by using direct methods and refined by full-matrix least-squares refinement. The Mo, O, P, and N atoms were refined anisotropically and the remaining atoms refined isotropically. $R = 0.024$, $R_w = 0.031$, GOF = 1.42. Highest peak on the final difference Fourier map was 1.26 e/Å^3. All computations were performed by using TEXSAN (TEXRAY structure analysis package, Molecular Structure Corp., 1985).

(4) Weight loss by thermogravimetric analysis: 22.5% calcd; 22.2% obsd. Bulk element anal. calcd: Mo, 42.35; P, 6.84; C, 15.91; H, 3.56; N, 3.09. Found: Mo, 41.99; P, 5.78; C, 16.42; H, 3.82; N, 3.20.

(5) Haushalter, R. C. *J. Chem. Soc., Chem. Commun.* **1987**, 1566.

0020-1669/90/1329-0157$02.50/0